metals

MDPI

Article

Microstructure and Shear Strength of SiC Joint Brazed with $LiAlSiO_4$ Reinforced AgCuTi Composite Filler

Jian Jiang, Gang Wang *, Mengmeng Wang and Yu Zhao

Anhui Key Laboratory of High-Performance Non-Ferrous Metal Materials, Anhui Polytechnic University, Wuhu 241000, China

* Correspondence: gangwang@ahpu.edu.cn

Abstract: In this work, SiC ceramics were successfully brazed at 900 °C using a composite brazing filler, and the effects of holding time and $LiAlSiO_4$ addition on the interfacial microstructure and mechanical properties of the joints were systematically investigated. The results showed that the brazed joints were devoid of obvious defects, and the joint structure was mainly composed of SiC/Ti_5Si_3/TiC + $TiCu_2$ + TiO_2 + LAS + $LiAlSi_2O_6$ + Cu (s, s) + Ag (s, s)/Ti_5Si_3/TiC/SiC. When the brazing temperature was 900 °C for 10 min and the $LiAlSiO_4$ addition was 1 wt%, the SiC brazed joints reached a maximum shear strength of 106.47 MPa, which was 4.7 times higher than that of the joints without $LiAlSiO_4$ addition under the same conditions. According to theoretical calculations, the addition of LAS can successfully reduce residual stresses in SiC brazed joints and enhance the joint strength.

Keywords: brazing; $LiAlSiO_4$; AgCuTi filler; residual stress

check for updates

Citation: Jiang, J.; Wang, G.; Wang, M.; Zhao, Y. Microstructure and Shear Strength of SiC Joint Brazed with $LiAlSiO_4$ Reinforced AgCuTi Composite Filler. *Metals* **2023**, *13*, 736. https://doi.org/10.3390/met13040736

Academic Editors: Alireza Akhavan-Safar and Aleksander Lisiecki

Received: 6 February 2023
Revised: 2 April 2023
Accepted: 6 April 2023
Published: 9 April 2023

Copyright: © 2023 by the authors. Licensee MDPI, Basel, Switzerland. This article is an open access article distributed under the terms and conditions of the Creative Commons Attribution (CC BY) license (https://creativecommons.org/licenses/by/4.0/).

1. Introduction

SiC ceramic is widely used as an important structural element in space reflector mirror blank materials [1], ballistic armor materials [2], electronic packaging [3], and nuclear fuel casing materials [4] due to its excellent mechanical strength, elastic modulus, wear resistance, thermal conductivity, and corrosion resistance [5–9]. However, the brittleness of SiC makes it difficult to fabricate large and complicated SiC-based components, which severely restricts the use of SiC-based materials. Therefore, developing a trustworthy joining method for SiC is a crucial issue for increasing its applications.

Presently, solid-state diffusion bonding [10], brazing [11], pressureless glass–ceramic joining [12], transient liquid phase welding [13], and MAX phase joining [14] are the primary SiC joining techniques. Because of its economic cost, easy implementation, and high-quality joining results, the brazing method has found widespread use in the aeronautics and space industries [15]. However, the large difference in the coefficient of thermal expansion (CTE) between SiC ceramics and brazing alloys is the main cause of cracks inside the reaction layer that impair the joint integrity. Adding low CTE materials into the brazing alloys has been proved successful in relieving the residual stress induced by the CTE mismatch to enhance the joint strength [16].

Negative expansion materials are a type of material with average linear expansion coefficients and bulk expansion coefficients that are negative across a specific temperature range [17]. Common materials with negative expansion include $LiAlSiO_4$ [18], $ZrV_{2-x}P_xO_7$ [19], ZrW_2O_7 [20], tungstate and molybdate series [21], etc. In recent years, researchers have begun to use materials with a negative expansion coefficient into brazing. Xue et al. [22] used AgCuTi filler with added Mo particles to reduce residual stress and CTE mismatch in SiC ceramics and Nb521 alloy brazing. The resulting AgCuTi + 5 wt% Mo filler exhibited a shear strength of ~78.5 MPa, which was 1.18 times greater than that of the AgCuTi filler alone. Similarly, Ba et al. [23] relieved the high residual stress in

C/SiC and Ti6Al4V brazed joints by adding ZrP_2WO_{12}(ZWP) particles to AgCu filler. The addition of 3 wt% ZWP particles effectively increased the shear strength of the joints to ~146.2 MPa, approximately 70.8% higher than that of joints without ZWP. Finite element analysis showed that the addition of 3 wt% ZWP reduced residual stress on the C/SiC side by 52.9 MPa. Wang et al. [24] developed a novel composite brazing alloy by adding negative thermal expansion $Y_2Mo_3O_{12}$ particles into an AgCuTi alloy to reduce the residual stress of the C_f/SiC-GH3536 joint. The negative thermal expansion behavior of $Y_2Mo_3O_{12}$ material and its effects on the shear strength of brazed joints were investigated. The shear strength of the C_f/SiC-GH3536 joints was able to reach ~42 MPa after the addition of 3 wt% $Y_2Mo_3O_{12}$, which is 1.6 times higher than without the addition of $Y_2Mo_3O_{12}$.

LAS is widely used in the fabrication of low-expansion ceramics, microcrystalline glass, metal matrix, and other composites due to its large negative coefficient of thermal expansion ($\alpha = -6.1 \times 10^{-6}$ K^{-1}), low density (2.67 g/cm^3), good thermal shock resistance, dielectric properties, and infrared radiation [25]. By compounding with other materials, it is possible to fabricate composites with negative or near-zero thermal expansion, which considerably improves the coefficient of thermal expansion and dimensional stability and prolongs the life of the materials. Jiang et al. [26] successfully bonded AlON ceramics to Ti_2AlNb by brazing and discovered that the addition 2 wt% LAS to AgCuTi brazing material at 860 °C for 10 min of holding time can achieve a maximum shear strength of 96.1 MPa, which is 248% of the strength of the joint without the addition of LAS. The residual stress in the joint is measured via Raman spectra, and the addition of LAS could lower the residual stress by up to 12.9%.

In this study, a new method to improve the application of reinforced phases is proposed, which provides a new method for the development of negative thermal expansion materials-reinforced metal composites. SiC ceramics were brazed using a novel composite filler alloy, which was AgCuTi filler alloy modified by adding LAS. In addition, the typical interfacial microstructure was characterized, the holding time and the effects of the LAS contents on the interfacial microstructure and shear strength of SiC brazed joints were analyzed in detail.

2. Materials and Methods

Prior to brazing, SiC ceramics were cut into 4 mm × 4 mm × 4 mm blocks using a diamond wire cutter, then the SiC ceramics ultrasonically cleaned in ethanol for 15 min. The Ag26.7Cu4.5Ti (wt%) active metal brazing powder was supplied by Changsha Tianjiu Metal Materials Co., Ltd. (Changsha, China), and the $LiAlSiO_4$ was supplied by the Zibo Chendong New Material Company. The average particle size of the powder was ~2 μm. The Ag26.7Cu4.5Ti (wt%) powder was compressed into tablet form using a tablet press. Subsequently, the $LiAlSiO_4$ powder was doped at 0.5 wt%, 1 wt%, 2 wt%, and 3 wt%, respectively. As shown in Figure 1a, the prepared brazing filler and the base material were assembled and then placed in the welding mold. The assembled samples were put into vacuum brazing equipment and heated until the vacuum degree was lower than 2.8×10^{-4} Pa. Figure 1b shows the brazing procedure.

The microstructure of the joints was analyzed using SEM (Hitachi SU8010, Hitachi Ltd., Tokyo, Japan) equipped with EDS (Thermo Ultradry SDD, Thermo Fisher Scientific Waltham, MA, USA). To improve conductivity before observation, a thin layer of gold was plated on the sample surface. The reactant phases were identified using an X-ray diffractometer (XRD, D-MAX Rapid II, RIGAKU, Tokyo, Japan) with Cu Kα radiation, operating at 5.4 kW with a diffracted beam diameter of 100 μm, a scanning range angle (2θ) of 20°~80°, and a scanning speed of 2°/min. To further investigate the micromorphology and phase composition of the joints, transmission electron microscopy (TEM, Tecnai F30, FEI, Hillsboro, OR, USA) combined with selected area electron diffraction (SAED), was used. The specimens for TEM observation were machined using a focused ion beam system (FIB, Scios 2 DualBeam, Thermo Fisher Scientific, Waltham, MA, USA). The shear strength of the joints was measured using an electro-mechanical universal testing machine (MTS

CMT4204, MTS, Shenzhen, China) with a loading rate of 0.5 mm/min. To ensure the measurement reliability, at least 3 specimens were tested for each test. Figure 1c shows a schematic diagram of the shear test.

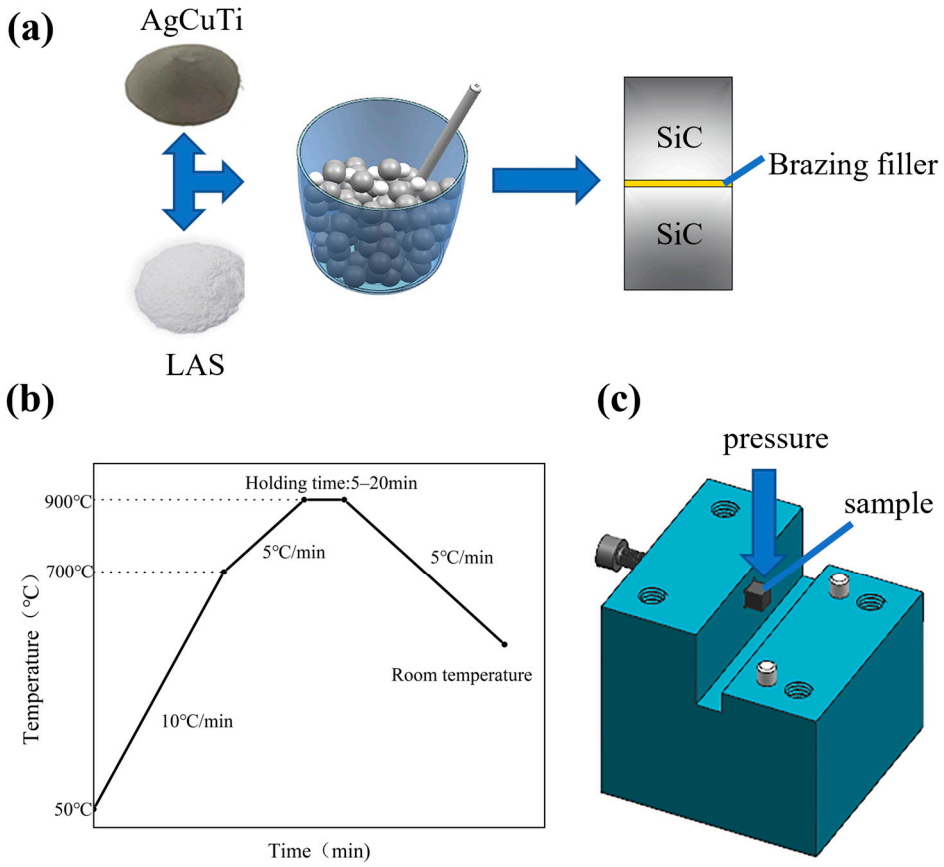


Figure 1. Schematic diagrams of (**a**) the assembly mode of brazing samples, (**b**) the curve of brazing process parameter and (**c**) shear strength test.

3. Results and Discussion

Figure 2 shows a typical joint interface for brazing SiC with pure AgCuTi at 900 °C for 10 min. It can be seen from Figure 2a that the AgCuTi filler reacts with the substrates on both sides and no obvious defects can be found in the joint. A partial enlargement of the brazed joint is seen in Figure 2b. The AgCuTi brazed SiC joint interface may be divided into three regions based on the microstructure of brazing joint: (I) the SiC zone, (II) interfacial reaction layer with an average thickness of ~4 μm adjacent to SiC and two identified phases marked as A and B; and (III) the middle zone of the weld with two identified phases marked as C and D. Figure 3b–f shows element distributions of the joint. The C from SiC ceramics are mainly concentrated on the ceramic side and tend to diffuse toward the middle of the joint. The Ti from the filler is enriched on the SiC side. The Ag and Cu from the filler were massively diffused and distributed in the whole joint.

The chemical compositions of phases A–D in the brazed joint are tabulated in Table 1. Ti and Si stay in phase A with an approximate atomic ratio of 5:3; it is inferred that phase A is Ti_5Si_3. The atomic percentage of the Ti element and C element in phase B is approximately 1:1; and thus, it is inferred that phase B is TiC. The light gray phase C is primarily composed of Cu elements; therefore, it is inferred that phase C is a Cu-based solid solution. The white phase D is an Ag-rich phase; the atomic content of Ag element reaches 83.97%. Thus, phase D is inferred to be an Ag-based solid solution.

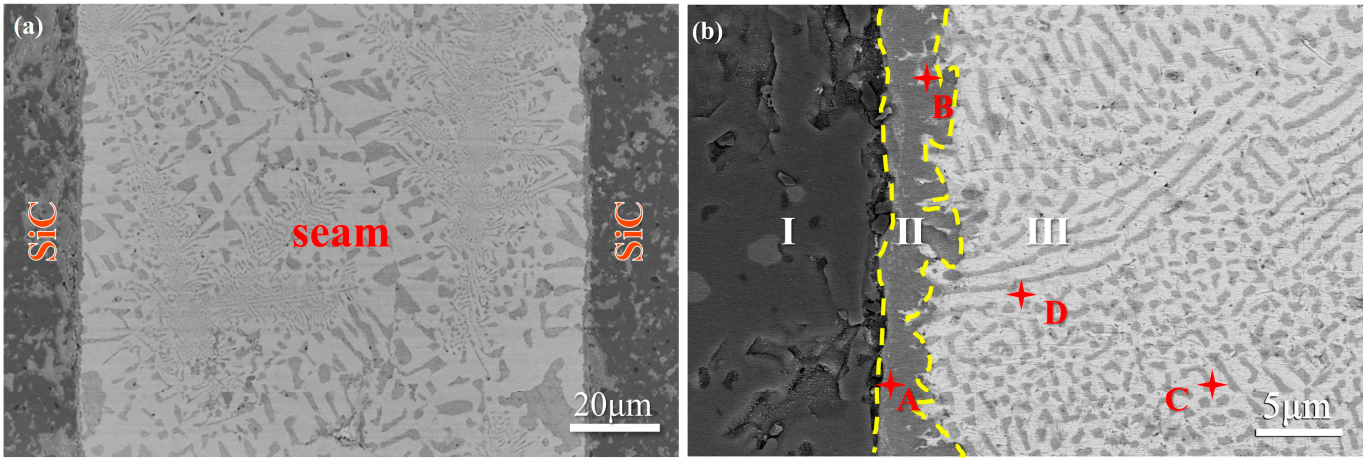


Figure 2. The SEM images of SiC joints brazed with pure AgCuTi at 900°C for 10 min (**a**) microstructure morphology of the whole brazing joint; and (**b**) local magnification of reaction layer.

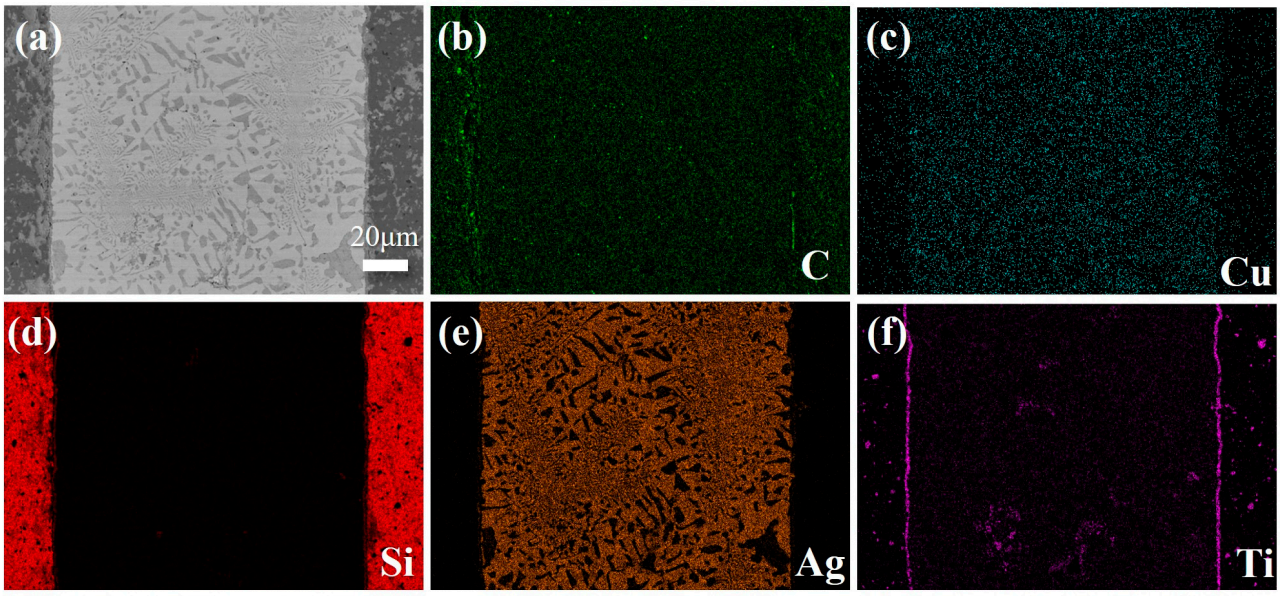


Figure 3. Microstructure and elemental distribution of SiC/AgCuTi/SiC joint brazed at 900 °C for 10 min (**a**) microstructure of joint, and (**b**–**f**) elemental distributions.

Table 1. The EDS analysis results of the various phases in the joint shown in Figure 2b (at. %).

Position	Ag	Cu	Ti	Si	C	Possible Phase
A	1.90	2.33	56.06	30.10	9.60	Ti_5Si_3
B	0.75	2.36	48.53	3.48	44.88	TiC
C	2.38	96.80	0.82	-	-	Cu (s, s)
D	83.97	14.92	1.11	-	-	Ag (s, s)

Figure 4 shows the typical microstructures of SiC joints brazed with AgCuTi/LAS composite material at 900 °C for 10 min. In Figure 4a, the joint is successfully brazed without any voids and cracks. As shown in Figure 4b, the brazing joints can be divided into three layers: layer I (the SiC side), layer II (the reaction layer at SiC side), and layer III (the brazing seam). Six mixed phases, marked A–F, were found in the zoomed image of a reaction layer at the SiC side. Figure 5b–h shows element distributions of the joint. The C from SiC ceramics is mainly concentrated on the ceramic side and tends to diffuse toward

the middle of the joint. The Ti from the filler is enriched on the SiC side. The Ag, Cu and Al from the filler are massively diffused and distributed in the whole joint.

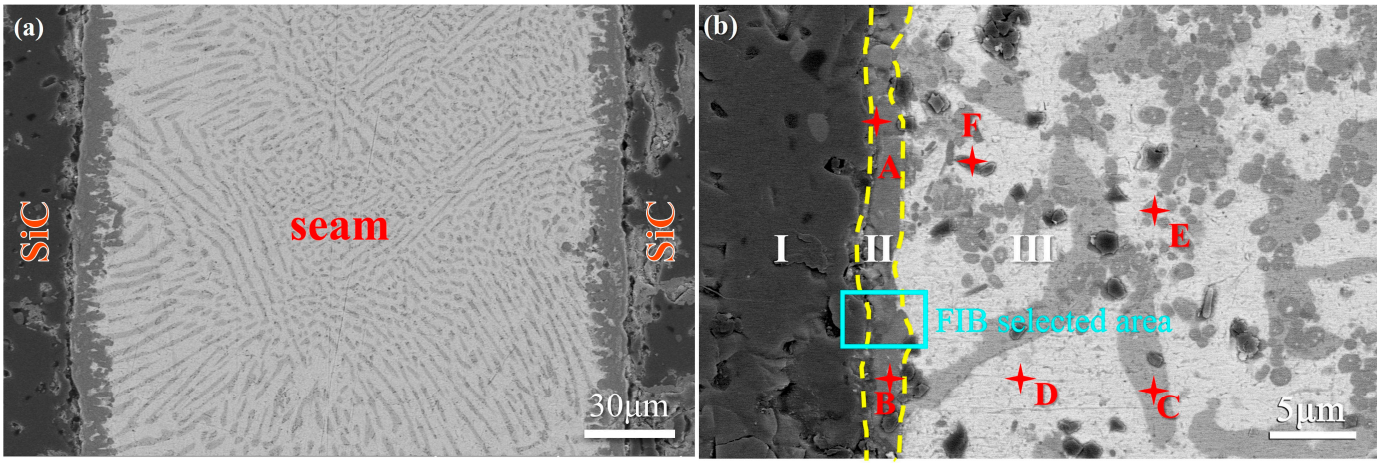


Figure 4. The SEM images of SiC joint brazed with AgCuTi + 1 wt% LAS composite brazing filler at 900 °C/10 min (**a**) microstructure morphology of the whole brazing joint; and (**b**) local magnification of reaction layer.

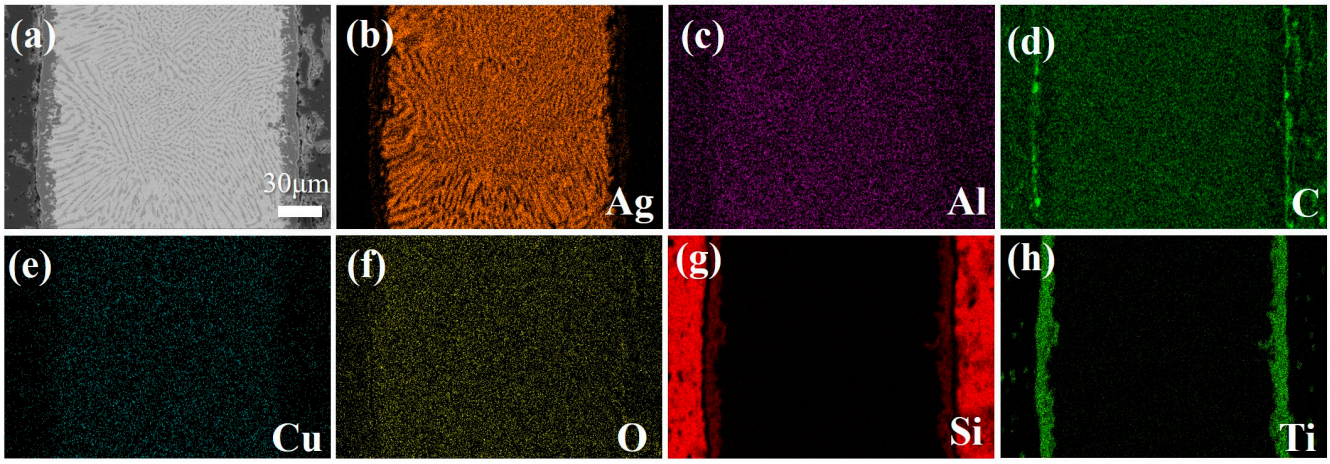


Figure 5. Microstructure and elemental distribution of SiC/AgCuTi + 1 wt% LAS/SiC joint brazed at 900 °C for 10 min (**a**) microstructure of joint, and (**b**–**h**) elemental distributions.

EDS is used to determine the element composition of the phase in different areas of the joint, which is shown in Figure 4b, and the results are listed in Table 2. Phase A is close to the SiC side, and phase B is close to the brazing filler side. Since the radius of Si is larger than the radius of C [27], the diffusion rate of Si in the AgCuTi brazing filler is smaller than C, and the main elements in the black phase A are Ti and Si with an approximate ratio of 5:3, it can be deduced that phase A may be the Ti_5Si_3 phase. The constituent elements of phase B are mainly Ti and C, and their ratio is about 1:1, so phase B may be the TiC phase. The main component of the light gray C phase is the Cu element, and the C phase is presumed to be a Cu-based solid solution. For phase D, the atomic content of the Ag element reaches 81.37%. Thus, phase D is inferred to be a Ag-based solid solution. The dark gray E phase is mainly distributed around the Cu-based solid solution, and its component elements are mainly Ti and Cu, combined with the atomic percentage; phase E is presumed to be the $TiCu_2$ phase. Phase F of the black particles is mostly composed of Si, Al, and O as its component constituents. It is reasonable to suppose that phase F is $LiAlSiO_4$.

Table 2. The EDS analysis results of the various phases in the joint shown in Figure 4b (at. %).

Position	Ag	Cu	Ti	Si	C	Al	O	Possible Phase
A	3.07	4.80	54.1	26.51	11.53	-	-	Ti_5Si_3
B	3.72	5.49	47.66	0.81	42.32	-	-	TiC
C	1.38	94.91	1.79	-	-	-	-	Cu (s, s)
D	81.37	16.63	2.00	-	-	-	-	Ag (s, s)
E	6.09	47.50	26.16	8.55	11.7	-	-	$TiCu_2$
F	1.38	1.27	1.79	29.61	-	22.05	43.91	$LiAlSiO_4$

In order to reveal the micro-structures and phase composition of the joint, TEM and the selected area electron (SEAD) patterns of zone II in Figure 4b were analyzed as shown in Figure 6. The reaction layer of the SiC/SiC brazed joint consists mainly of Ti elements; Al elements are diffusely distributed near the reaction layer, Si elements are primarily distributed on both sides of the reaction layer, and Cu and Ag elements are alternately distributed on the right side of the reaction layer. Figure 6g shows the TEM analysis of $LiAlSi_2O_6$, which is consistent with the result of Zhang [28]; part of the $LiAlSi_2O_6$ was formed via the reaction of $2LiAlSiO_4 \rightarrow LiAlSi_2O_6 + LiAlO_2$. Figure 6h shows the TEM analysis of $TiCu_2$, which is consistent with the results of the EDS analysis. The spot was identified as diffraction from the $[41\bar{3}]$ zone axis for TiO_2 as shown in Figure 6i.

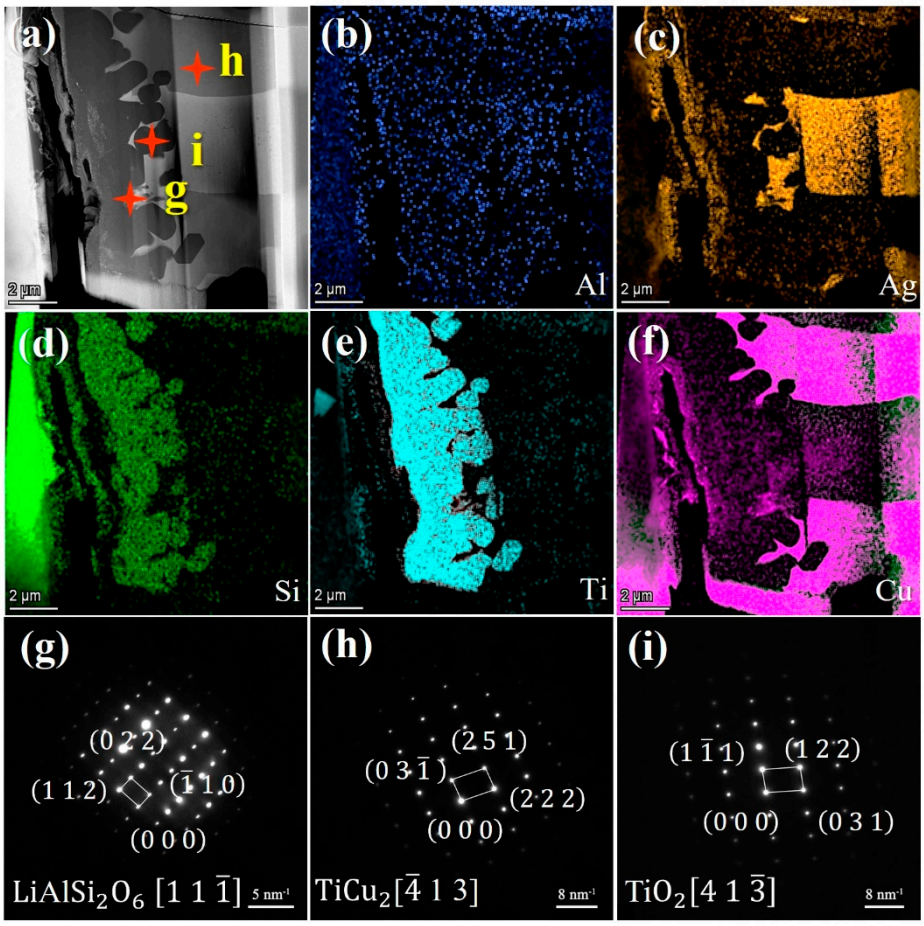


Figure 6. (**a**) HAADF images of SiC joints brazed with AgCuTi + 1 wt% $LiAlSiO_4$ at 900 °C for 10 min; (**b**–**f**) elemental distributions corresponding to Al, Ag, Si, Ti, Cu; (**g**–**i**) selected area electron diffraction (SAED) patterns corresponding to the three points in figure (**a**).

Figure 7 shows the micro-focused XRD patterns of SiC joints brazed with different LAS content reinforced AgCuTi brazing fillers, and the four XRD patterns from bottom to

top represent the doping amounts of 0.5 wt%, 1 wt%, 2 wt%, and 3% LAS, respectively. It can be observed that the four groups of SiC joints with different LAS doping are mainly composed of Cu (s, s), Ag (s, s), Ti_5Si_3 and $TiCu_2$. In summary, under the conditions of brazing temperature of 900 °C for 10 min, the SiC joints were brazed well, and the typical microstructure of the joint could be described as SiC/Ti_5Si_3/TiC + $TiCu_2$ + TiO_2 + LAS + $LiAlSi_2O_6$ + Cu (s, s) + Ag (s, s)/Ti_5Si_3/TiC/SiC.

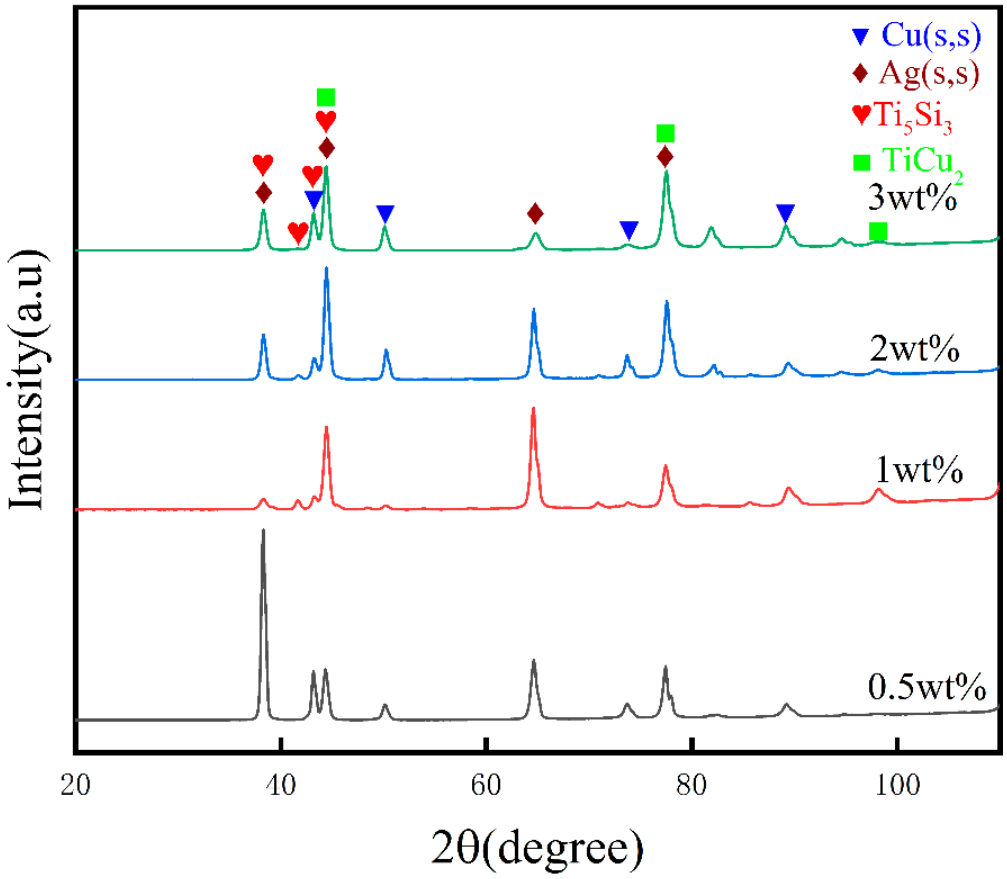


Figure 7. XRD patterns of micro-zones of brazed SiC joints with AgCuTi and different $LiAlSiO_4$ doping at 900 °C/10 min.

From the above analysis, in order to systematically investigate the formation mechanism of SiC joints brazed with AgCuTi/LAS composite brazing filler, a physical model is established, and the diagram of the brazed joint is visualized in Figure 8. The formation of brazed joints can be divided into four stages as follows. Before brazing, the AgCuTi/LAS interlayer is added into the brazing seam. The SiC ceramics, AgCuTi/LAS interlayer, and SiC ceramics are assembled into a sandwich structure. In the first stage, as shown in Figure 8a, when the brazing temperature is under the melting point of the composite brazing filler, the plastically deformed filler is in tight contact with the SiC. Due to the large difference in electronegativity between Si, C and Ti [29], the Ti in the brazing material have a tendency to diffuse to the SiC on both sides.

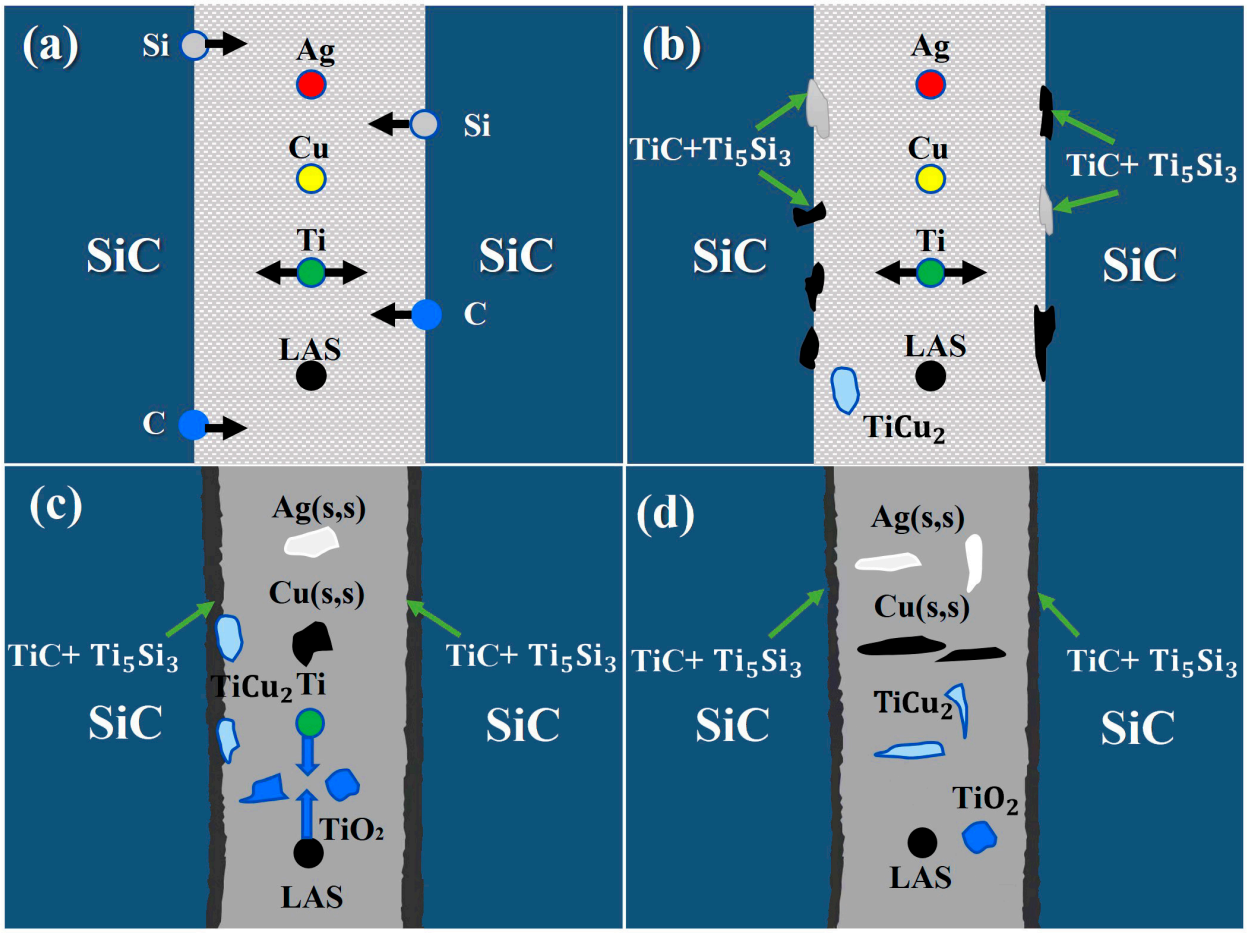


Figure 8. Schematic diagram of the microstructure evolution of SiC brazed joints. (**a**) solid phase diffusion during the physical contact stage, (**b**) atomic diffusion during melting of filler metal, (**c**) interface reaction during heat preservation, (**d**) products formation after cooling.

In the second stage, the brazing temperature reaches the melting point of the AgCuTi brazing filler as shown in Figure 8b. When the concentration of Ti elements reaches the critical concentration for the interfacial reaction, at the SiC ceramic side, a reaction of $5Ti + 3Si \rightarrow Ti_5Si_3$ occurs due to the lowest Gibbs free energy of Ti_5Si_3 [30]. The negative Gibbs free energy of TiC induces the reaction of Ti and C in the composite filler to produce TiC by $Ti + C \rightarrow TiC$ [31]. At this stage, the Ti elements are combined with SiC to form the TiC interfacial barrier layer [32], which hinders the interfacial reaction between the AgCuTi active filler and LAS. With an increase in reaction time, the interaction of Ti and SiC reduces the Ti concentration on the joint, resulting in the diffusion of Ti to the joint interface to form TiC and Ti_5Si_3, which form a discontinuous and thinner reaction layer. Since the radius of Si is greater than that of C [33], the diffusion rate of Si in the AgCuTi composite brazing filler is less than that of C, and the formed Ti_5Si_3 phase is nearer to the intermediate brazing seam side. The formation of TiC with Ti_5Si_3 can be evidenced in the EDS analysis results in Table 2.

In the third stage, as shown in Figure 8c,d, the $TiCu_2$ phase, which is spread in an island-like pattern on the front side of the reaction layer, is formed via the reaction of $Ti + 2Cu \rightarrow TiCu_2$ in the middle of the joint, and the addition of LAS promotes the transformation of Ti-Cu compounds into $TiCu_2$ due to Ti being consumed by LAS [34]. As the holding time increases, the thickness of the reaction layer increases, and the formation of a continuous reaction layer inhibits the further diffusion of Si and C into the brazing material at the interface. The TiC barrier layer helps to reduce the interfacial reaction and make the LAS exert the negative thermal expansion effect fully [35]. At this time,

the main reaction between Ti and O in the LAS undergoes a process of Ti + 2O → TiO_2. Based on the analysis of the TEM results, the presence of $TiCu_2$ and TiO_2 in the joint can be confirmed. With the extension of the holding time, the size of the AgCu eutectic structure is reduced. Following the further decrease in temperature, no other phase is precipitated from the molten.

The holding time in the brazing process is an important factor that affects the interfacial structure and strength of the joint. The effects of holding time on the microstructure of SiC/AgCuTi + 1 wt% LAS/SiC brazed joints were investigated. Microstructures of the joint brazed at 900 °C for 5~20 min are shown in Figures 9 and 10. With the extension of the holding time, the size of the AgCu eutectic structure is reduced. When the holding time is 5 min, the width of the brazing seam is ~150 μm, and the thickness of the reaction layer is about ~5 μm. Due to the short holding time, large Cu-based solid solutions are present in the joint. When the holding time increases to 10 min, as shown in Figure 10b, the thickness of the reaction layer increases to ~7 μm. When the holding time increases to 20 min, the interfacial microstructure of the joint is shown in Figures 9d and 10d. The thickness of the reaction layer decreases to ~2 μm. The possible reason for this phenomenon is that the added LAS consumed more Ti in the original filler, resulting in the concentration reduction in Ti, which reacted with SiC.

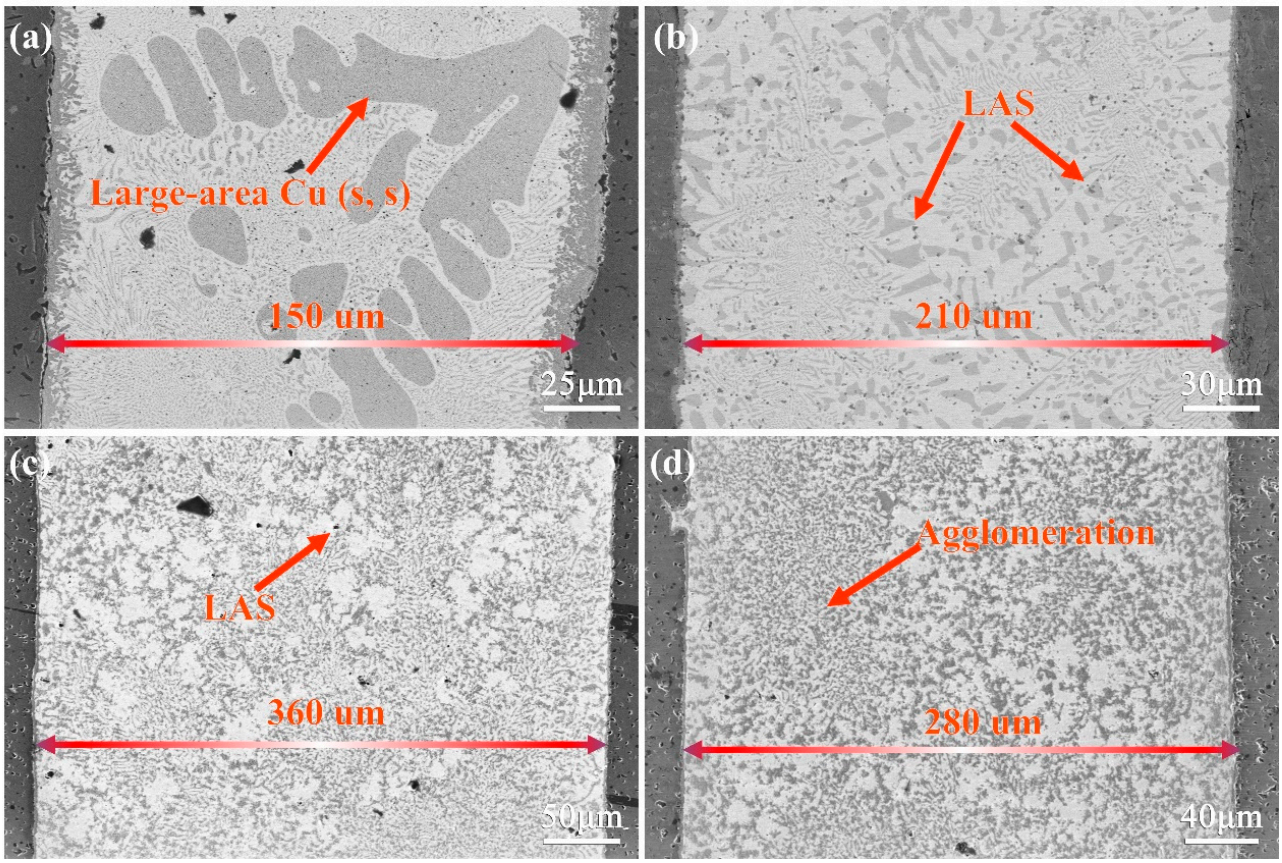


Figure 9. Typical interfaces of AgCuTi + 1 wt% $LiAlSiO_4$ brazed SiC joints with different holding times at 900 °C; (**a**–**d**) holding times 5 min, 10 min, 15 min, and 20 min, respectively.

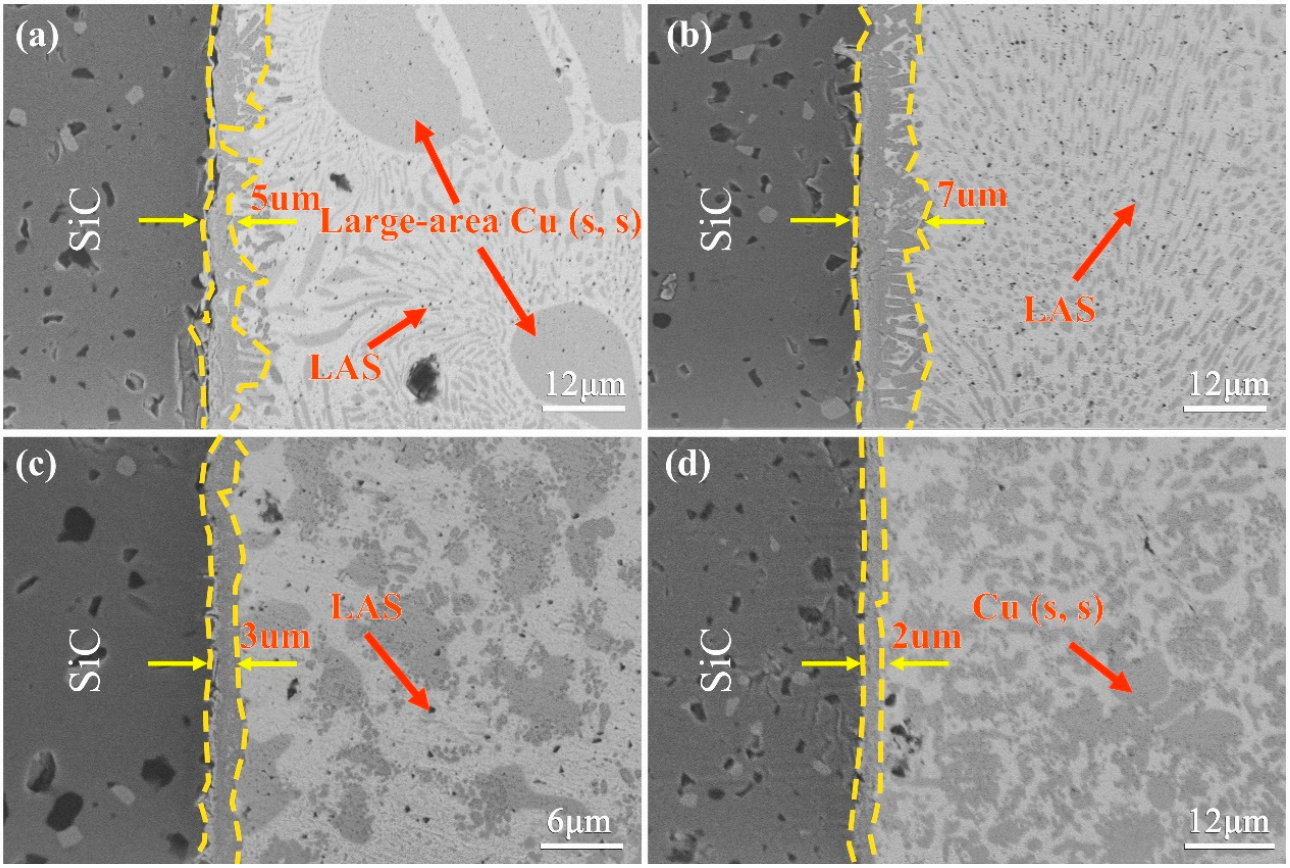


Figure 10. Local enlargement of typical interfaces of AgCuTi + 1 wt% $LiAlSiO_4$ brazed SiC joints with different holding times at 900 °C; (**a**–**d**) holding times 5 min, 10 min, 15 min, and 20 min.

To study the effect of the content of LAS on the microstructure and mechanical properties of SiC joint, LAS enhanced AgCuTi composite fillers with LAS content of 0.5 wt%, 1 wt%, 2 wt% and 3 wt% were used to establish the joining of them with the same holding time. Figures 11 and 12 depict the interfacial structure of the joints with different LAS contents and the local magnification of the reaction layer at 900 °C for 10 min. When pure AgCuTi filler was adopted as shown in Figures 11a and 12a, the brazed seam was mainly composed of AgCu eutectic. The reaction layer was dense and was around ~2.5 μm thick. The size of the AgCu eutectic structure was reduced when the LAS content in the composite filler was 1 wt% as shown in Figure 11c, indicating that more LAS was favorable for the structure of dispersive distribution. The thickness of the reaction layer was around ~7 μm as shown in Figure 12c. Further increase in LAS content to 2 wt% led to the aggregation of Ag-Cu eutectic at the interface as shown in Figure 11d. Another significant variety was that LAS phases almost disappeared, and the reaction layer thickness was reduced to approximately ~2.5 μm. The reduction in the thickness of the reaction layer may be due to the full reaction of the added LAS with Ti. Further increasing the LAS content to 3 wt%, holes could be easily found in the brazed seam as shown in Figure 11e. The agglomerate of Ag-Cu eutectic led to defects in the joints, which negatively affected joint performance [36]. It is noteworthy that the thickness of the reaction layer changed little. In such a situation, the microstructure variation of the brazed seams plays a decisive role on the mechanical performance of the joint.

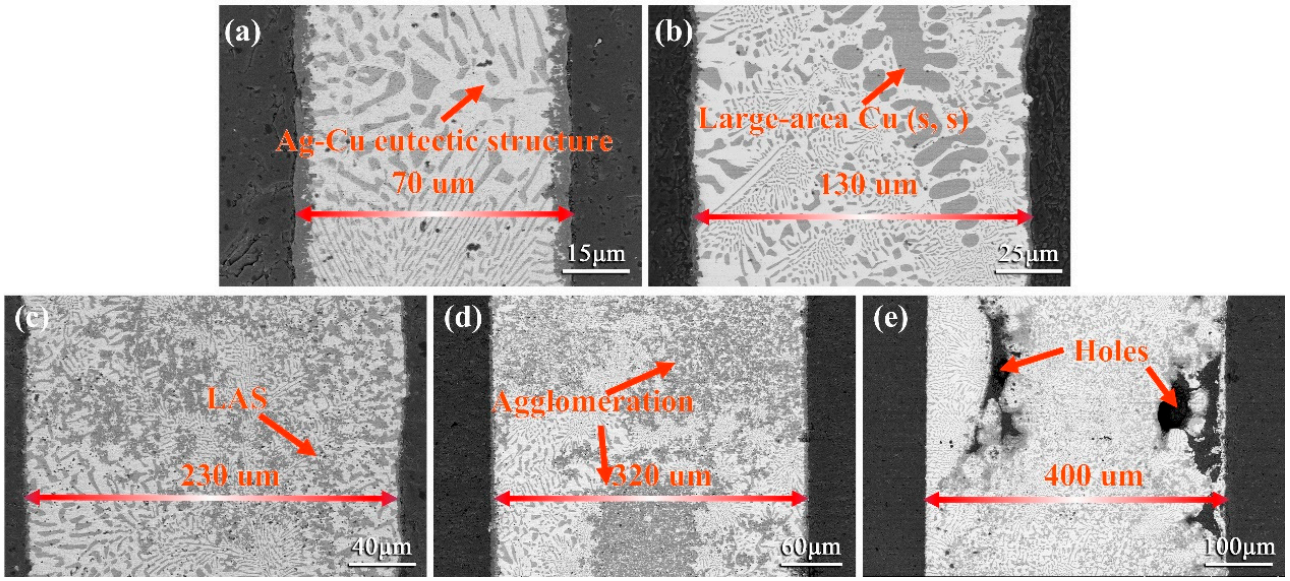


Figure 11. Typical overall morphology of the interface of SiC joints brazed with AgCuTi composite brazing filler at 900 °C for 10 min; (**a**–**e**) LAS additions of 0 wt%, 0.5 wt%, 1 wt%, 2 wt%, and 3 wt%, respectively.

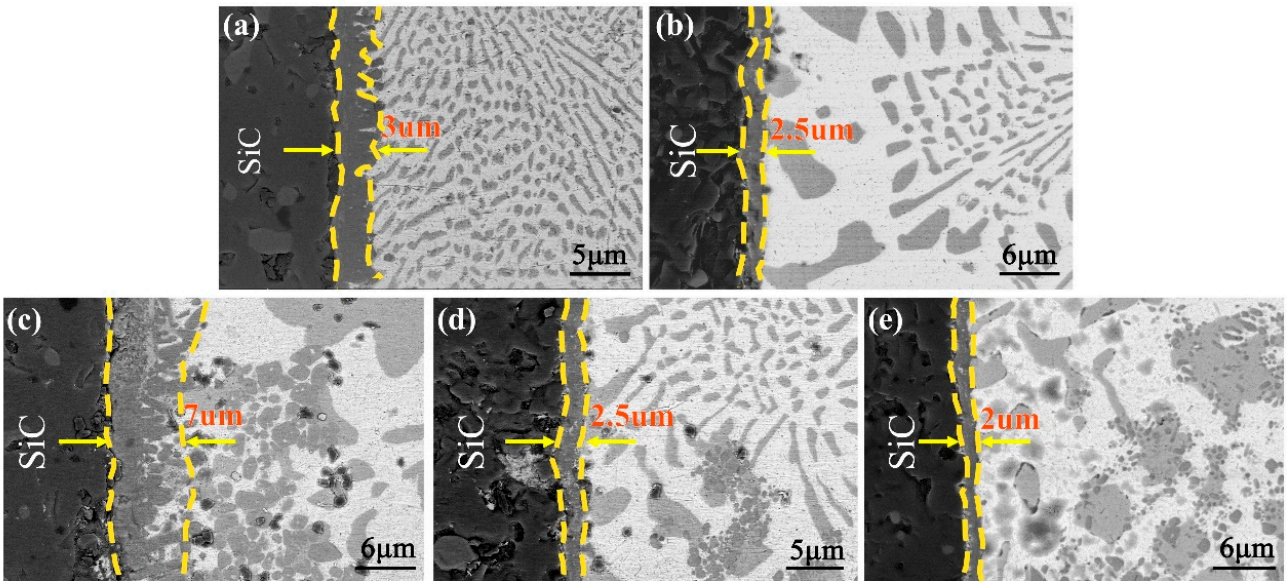


Figure 12. Local enlargement of typical interface of AgCuTi composite brazing filler brazing SiC joints at 900 °C for 10 min; (**a**–**e**) LAS additions of 0 wt%, 0.5 wt%, 1 wt%, 2 wt%, and 3 wt%, respectively.

The joint shear strength of AgCuTi + 1 wt% $LiAlSiO_4$ with different holding times at 900 °C is shown in Figure 13a. Initially, the joint shear strength is low when the holding time is short due to the insufficient reaction between the ceramic and the brazing filler. However, with increasing the holding time, the reaction becomes more adequate, resulting in improved joint strength. Nonetheless, further extension of the holding time leads to an increase in the thickness of the Ti_5Si_3 brittle reaction layer [37], which raises the strain energy of the joint and consequently weakens its strength [38]. As a result, the strength of the joint initially increases and then decreases as the holding time is prolonged. The highest strength of the joint, which is 106.47 MPa, is achieved when the holding time is 10 min.

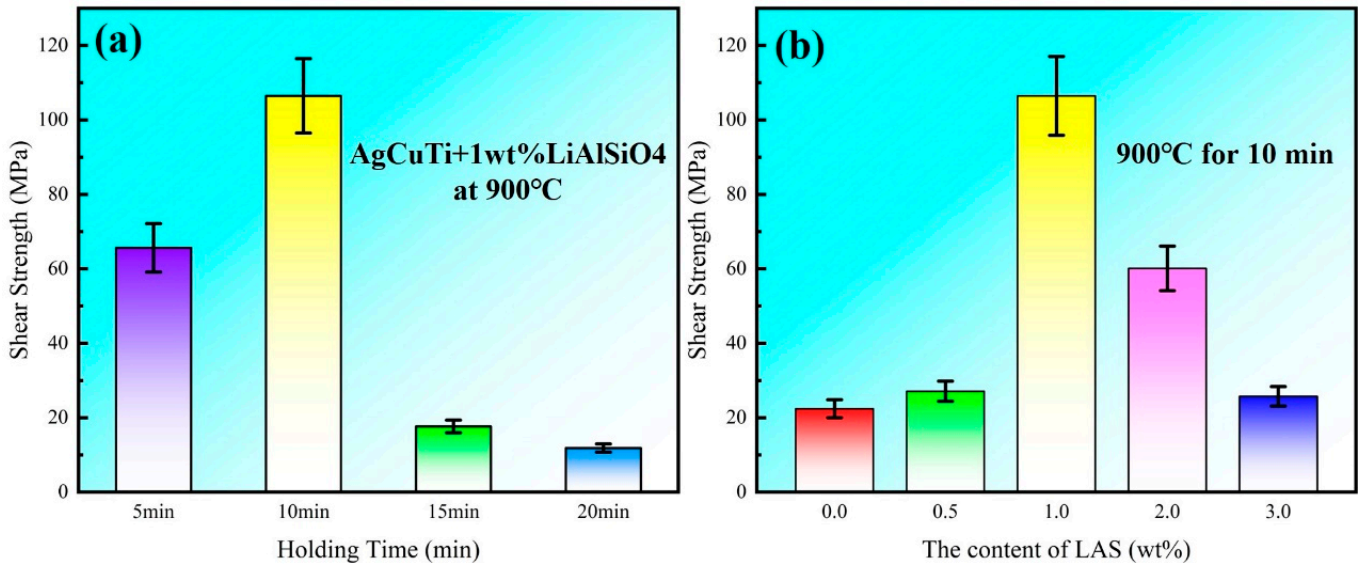


Figure 13. The effect of (**a**) holding time and (**b**) LAS content on the shear strength of SiC joints.

In Figure 13b, the shear strength of a joint brazed with different contents of LAS-strengthened AgCuTi filler at 900 °C for 10 min is shown. The use of composite filler improved the shear strength of the joint compared to pure AgCuTi filler. The maximum shear strength of 106.47 MPa was achieved when the LAS content was 1 wt%, which is 85 MPa higher than when pure AgCuTi filler was used. However, the shear strength decreased sharply when the LAS content was increased to 2 wt% or 3 wt%. This can be attributed to the fact that when the LAS content is low, the effect of LAS to relieve the mismatch between AgCuTi brazing material and SiC ceramic CTE is not significant, leading to high residual stress in the joint. On the other hand, excessive LAS will react vigorously with Ti, generating more TiO_2 and other phases. These phases have high melting points and uneven distribution, which can lead to the accumulation of more residual stress at the brazed joint [39], resulting in degraded properties of the joint. The addition of LAS in the filler alloy reduced the CTE in the joint, releasing the residual stress and improving the joining quality. However, excessive reinforcing particles in the alloy reduced the fluidity of the liquid composite filler [40], while excessive LAS near the SiC substrate reduced the active Ti content, resulting in insufficient reactions between the Ti and SiC substrate, leading to poor wettability and connectivity of the brazing layer to the SiC substrate. Therefore, a suitable LAS content of 1 wt% was found to be essential and reasonable.

To further investigate the effect of the microstructure of the seam and the residual stress caused by the difference in the CTE between the metal and the ceramic on the shear strength of the brazed joint, the residual stress on the SiC side can be calculated using Equation (1) as follows [41], and the basic properties of materials used in the computations are given in Table 3:

$$\sigma = \frac{E_c E_m}{E_c + E_m}(\alpha_c - \alpha_m)\Delta T \quad (1)$$

where E_c and E_m are the modulus of elasticity of the base material and brazing material, respectively; α_c and α_m are the CTE of the base material and brazing material, respectively; and ΔT is the difference between brazing temperature and room temperature. According to Equation (1), the residual stress of the brazed joint is estimated to be −0.794 GPa. When LAS is added to AgCuTi to relieve the residual stress, the brazing material is changed to the AgCuTi/LAS composite brazing material, and its elastic modulus and thermal expansion coefficient can be calculated according to Equations (2) and (3) [32], respectively:

$$E = E_m \left[1 - \frac{3V_f \left(E_f - E_m \right)}{\left(E_f - E_m \right) \left(1 - 2V_f \right) + 3E_m} \right]^{-1} \quad (2)$$

$$\alpha = \alpha_m - \frac{3V_f E_f \left(\alpha_m - \alpha_f \right)}{\left(E_f - E_m \right) \left(1 + 2V_f \right) + 3E_m} \quad (3)$$

where E is the elastic modulus of the composite brazing material, E_m is the elastic modulus of the matrix, V_f is the volume fraction of the reinforced phase, i.e., the percentage of the reinforced phase in the total volume, which can be estimated as 0.29. E_f is the elastic modulus of the reinforcing phase, α is the CTE of the composite brazing material, α_m is the CTE of the matrix, and α_f is the CTE of the reinforcing phase. According to Equations (2) and (3), the elastic modulus of the SiC/AgCuTi + LAS/SiC brazed joint was calculated as 66.134 GPa, and the weld residual stress on the SiC side was 1.3×10^{-5} GPa. Comparing with the pure AgCuTi brazing filler, it can be concluded that LAS as the reinforcing phase can effectively reduce the residual stress in the joint.

Table 3. Basic properties of materials used in the computations [42].

Material	Temperature (°C)	Yield Strength (MPa)	Density (g/cm^3)	Poisson's Ratio	Elastic Modulus (GPa)	CET ($\times 10^{-6}$ K^{-1})
SiC	900	300	3.1	0.2	420	4.8
AgCuTi		20	9.76	0.363	67	20.5
LAS		190	2.67	0.25	64	−6.1

4. Conclusions

In this paper, AgCuTi/LAS is selected as the composite filler for brazing SiC ceramics under different technological parameters. The effects of holding time on the microstructure and properties of the joint were explored. The primary conclusions are as follows:

(1) When brazing SiC joints with AgCuTi/LAS composite brazing filler, the typical structure of the joints is SiC/Ti_5Si_3/TiC + $TiCu_2$ + TiO_2 + LAS + $LiAlSi_2O_6$ + Cu(s, s) + Ag(s, s)/Ti_5Si_3/TiC/SiC.

(2) The maximum shear strength of the joint at 900 °C for 10 min is 106.47 MPa when 1 wt% LAS is added. This value is 4.7 times greater than the condition without LAS. The Ag–Cu eutectic structure reduces in size and undergoes agglomeration with the extension of the holding time and the increase in the LAS addition.

(3) According to theoretical calculations, the addition of LAS can effectively reduce residual stresses in the SiC brazed joints. The residual stress is reduced from −0.794 GPa to 1.3×10^{-5} GPa with 1 wt% LAS addition.

Author Contributions: Conceptualization, J.J. and G.W.; methodology, J.J.; software, M.W.; writing—original draft preparation, J.J.; writing—review and editing, J.J. and G.W.; visualization, Y.Z. All authors have read and agreed to the published version of the manuscript.

Funding: This work was financially supported by the National Natural Science Foundation of China [52171148; 51704001], Natural Science Foundation of Anhui Province [2008085J23], Talent Project of Anhui Province [Z175050020001; gxyqZD2020059].

Data Availability Statement: Not available.

Conflicts of Interest: The authors declare no conflict of interest.

References

1. Li, D.; Li, H.; Li, B. A Novelty Design for Radiation Resistance of SiC by Recrystallization-Induced Stacking Faults. *J. Mater. Res. Technol.* **2022**, *19*, 3852–3856. [CrossRef]
2. Bhat, A.; Naveen, J.; Jawaid, M.; Norrrahim, M.N.F.; Rashedi, A.; Khan, A. Advancement in Fiber Reinforced Polymer, Metal Alloys and Multi-Layered Armour Systems for Ballistic Applications—A Review. *J. Mater. Res. Technol.* **2021**, *15*, 1300–1317. [CrossRef]
3. Zhu, G.; Feng, Q.; Yang, J.; Hu, J.; Wang, H.; Xue, Y.; Shan, Q.; Dong, S. Effect of BNNTs/Matrix Interface Tailoring on Toughness and Fracture Morphology of Hierarchical SiCf/SiC Composites. *J. Adv. Ceram.* **2019**, *8*, 555–563. [CrossRef]
4. Katoh, Y.; Ozawa, K.; Shih, C.; Nozawa, T.; Shinavski, R.J.; Hasegawa, A.; Snead, L.L. Continuous SiC Fiber, CVI SiC Matrix Composites for Nuclear Applications: Properties and Irradiation Effects. *J. Nucl. Mater.* **2014**, *448*, 448–476. [CrossRef]
5. Zhou, X.; Liu, J.; Zou, S.; Xu, K.; Chang, K.; Li, P.; Huang, F.; Huang, Z.; Huang, Q. Almost Seamless Joining of SiC Using an In-Situ Reaction Transition Phase of Y3Si2C2. *J. Eur. Ceram. Soc.* **2020**, *40*, 259–266. [CrossRef]
6. Lv, X.; Ye, F.; Cheng, L.; Fan, S.; Liu, Y. Fabrication of SiC Whisker-Reinforced SiC Ceramic Matrix Composites Based on 3D Printing and Chemical Vapor Infiltration Technology. *J. Eur. Ceram. Soc.* **2019**, *39*, 3380–3386. [CrossRef]
7. Qian, M.; Xu, X.; Qin, Z.; Yan, S. Silicon Carbide Whiskers Enhance Mechanical and Anti-Wear Properties of PA6 towards Potential Applications in Aerospace and Automobile Fields. *Compos. Part B Eng.* **2019**, *175*, 107096. [CrossRef]
8. Murayama, N.; Hirao, K.; Sando, M.; Tsuchiya, T.; Yamaguchi, H. High-Temperature Electro-Ceramics and Their Application to SiC Power Modules. *Ceram. Int.* **2018**, *44*, 3523–3530. [CrossRef]
9. Wan, P.; Li, M.; Xu, K.; Wu, H.; Chang, K.; Zhou, X.; Ding, X.; Huang, Z.; Zong, H.; Huang, Q. Seamless Joining of Silicon Carbide Ceramics through an Sacrificial Interlayer of Dy3Si2C2. *J. Eur. Ceram. Soc.* **2019**, *39*, 5457–5462. [CrossRef]
10. Sun, L.; Yang, Q.; Zou, J.; Ni, L.; Song, X.; Zhang, R.; Liang, S. Effect of Hot-Dip Tin Coating Treatment on the CuSn10Pb10/45 Steel Joint Fabricated by Diffusion Bonding. *J. Mater. Res. Technol.* **2022**, *18*, 1147–1154. [CrossRef]
11. Zhao, S.; Chen, H.; Nai, X.; Wang, P.; Deng, H.; Wen, G.; Liu, F.; Li, W. Effect of Ti Content on Microstructure and Mechanical Properties of SiCf/SiC Composites/GH536 Superalloy Joints Brazed with CoFeCrNiCuTi High Entropy Filler. *J. Manuf. Process.* **2023**, *85*, 132–140. [CrossRef]
12. Casalegno, V.; Kondo, S.; Hinoki, T.; Salvo, M.; Czyrska-Filemonowicz, A.; Moskalewicz, T.; Katoh, Y.; Ferraris, M. CaO-Al_2O_3 Glass-Ceramic as a Joining Material for SiC Based Components: A Microstructural Study of the Effect of Si-Ion Irradiation. *J. Nucl. Mater.* **2018**, *501*, 172–180. [CrossRef]
13. Wu, L.-X.; Lin, R.-L.; Niu, W.-B.; Zhu, L.-L.; Xue, J.-X.; Liao, Y.-H.; Liu, T.; Guo, W.-M.; Sun, S.-K.; Lin, H.-T. Nano-Infiltration and Transient Eutectic (NITE) Phase Joining SiC Ceramics at 1500 °C. *Ceram. Int.* **2019**, *45*, 24927–24931. [CrossRef]
14. Fitriani, P.; Septiadi, A.; Hyuk, J.D.; Yoon, D.-H. Joining of SiC Monoliths Using a Thin MAX Phase Tape and the Elimination of Joining Layer by Solid-State Diffusion. *J. Eur. Ceram. Soc.* **2018**, *38*, 3433–3440. [CrossRef]
15. Yang, J.; Huang, J.; Ye, Z.; Chen, S.; Ji, R.; Zhao, Y. Influence of Interfacial Reaction on Reactive Wettability of Molten Ag-Cu-X Wt.%Ti FIller Metal on SiC Ceramic Substrate and Mechanism Analysis. *Appl. Surf. Sci.* **2018**, *436*, 768–778. [CrossRef]
16. Song, X.; Li, H.; Zeng, X.; Zhang, L. Brazing of C/C Composites to Ti6Al4V Using Graphene Nanoplatelets Reinforced TiCuZrNi Brazing Alloy. *Mater. Lett.* **2016**, *183*, 232–235. [CrossRef]
17. Miller, W.; Smith, C.W.; Mackenzie, D.S.; Evans, K.E. Negative Thermal Expansion: A Review. *J. Mater. Sci.* **2009**, *44*, 5441–5451. [CrossRef]
18. Xu, H.; Heaney, P.J.; Navrotsky, A. Thermal Expansion and Structural Transformations of Stuffed Derivatives of Quartz along the $LiAlSiO_4$ -SiO_2 Join: A Variable-Temperature Powder Synchrotron XRD Study. *Phys. Chem. Miner.* **2001**, *28*, 302–312. [CrossRef]
19. Shi, N.; Song, Y.; Xing, X.; Chen, J. Negative Thermal Expansion in Framework Structure Materials. *Coord. Chem. Rev.* **2021**, *449*, 214204. [CrossRef]
20. Takenaka, K. Negative Thermal Expansion Materials: Technological Key for Control of Thermal Expansion. *Sci. Technol. Adv. Mater.* **2012**, *13*, 013001. [CrossRef]
21. Wang, T.; Ivas, T.; Lee, W.; Leinenbach, C.; Zhang, J. Relief of the Residual Stresses in Si_3N_4/Invar Joints by Multi-Layered Braze Structure—Experiments and Simulation. *Ceram. Int.* **2016**, *42*, 7080–7087. [CrossRef]
22. Xue, H.; Ding, Z.; Guo, W.; Luan, X.; Chen, C.; Jia, Y. Effect of Mo Addition on Residual Stress and Mechanical Properties of SiC Ceramic/Nb521 Alloy Joints Brazed by Using AgCuTi Filler. *Mater. Lett.* **2022**, *310*, 131500. [CrossRef]
23. Ba, J.; Zheng, X.H.; Ning, R.; Lin, J.H.; Qi, J.L.; Cao, J.; Cai, W.; Feng, J.C. C/SiC Composite-Ti6Al4V Joints Brazed with Negative Thermal Expansion ZrP2WO12 Nanoparticle Reinforced AgCu Alloy. *J. Eur. Ceram. Soc.* **2019**, *39*, 755–761. [CrossRef]
24. Wang, P.; Liu, X.; Wang, H.; Cao, J.; Qi, J.; Feng, J. Negative Thermal Expansion $Y_2Mo_3O_{12}$ Particles Reinforced AgCuTi Composite Filler for Brazing Cf/SiC and GH3536. *Mater. Charact.* **2022**, *185*, 111754. [CrossRef]
25. Reimanis, I.E.; Seick, C.; Fitzpatrick, K.; Fuller, E.R.; Landin, S. Spontaneous Ejecta from?-Eucryptite Composites. *J. Am. Ceram. Soc.* **2007**, *90*, 2497–2501. [CrossRef]
26. Jiang, H.; Li, C.; Mao, X.; Chen, L.; Zhao, W.; Si, X.; Qi, J.; Dong, Z.; Cao, J. Vacuum Brazing of AlON and Ti2AlNb with $LiAlSiO_4$ Enhanced Ag–Cu–Ti Composite Fillers: Microstructure, Mechanical Properties and Measurement of Residual Stress. *Mater. Sci. Eng. A* **2022**, *846*, 143277. [CrossRef]
27. Wang, G.; Yang, Y.; Wang, M.; He, R.; Tan, C.; Cao, W.; Xu, H. Brazing ZrB2-SiC Ceramics to Nb with a Novel CoFeNiCrCu High Entropy Alloy. *J. Eur. Ceram. Soc.* **2021**, *41*, 54–61. [CrossRef]

28. Zhang, J.; Zhao, Y.; Xu, H.; Zelinskas, M.V.; Wang, L.; Wang, Y.; Uchida, T. Pressure-Induced Amorphization and Phase Transformations in β-$LiAlSiO_4$. *Chem. Mater.* **2005**, *17*, 2817–2824. [CrossRef]
29. Zhao, S.; Chen, H.; Nai, X.; Wang, P.; Deng, H.; Wen, G.; Liu, F.; Li, W. Microstructure and Mechanical Properties of SiCf/SiC Composites/ GH536 Superalloy Joints Brazed with CoFeNiCrCu High-Entropy Alloy Filler. *Mater. Charact.* **2022**, *194*, 112419. [CrossRef]
30. Li, X.; Wang, H.; Wang, T.; Zhang, B.; Yu, T.; Li, R. Microstructural Evolution Mechanisms of Ti600 and Ni-25%Si Joint Brazed with Ti-Zr-Ni-Cu Amorphous Filler Foil. *J. Mater. Process. Technol.* **2017**, *240*, 414–419. [CrossRef]
31. Wang, G.; Yang, Y.; Wu, P.; Shu, D.; Zhu, D.; Tan, C.; Cao, W. Effect of Brazing Temperature on Microstructure and Mechanical Properties of $TiAl/ZrB_2$ Joint Brazed with CuTiZrNi Filler. *J. Manuf. Process.* **2019**, *46*, 170–176. [CrossRef]
32. Wang, P.; Lin, J.; Xu, Z.; Qin, B.; Cao, J.; Feng, J.; Qi, J. Negative Thermal Expansion of $Sc_2W_3O_{12}$ Interlayer with Three-Dimensional Interpenetrating Network Structure for Brazing C/SiC Composites and GH3536. *Carbon* **2023**, *201*, 765–775. [CrossRef]
33. Liu, Y.; Wang, G.; Cao, W.; Xu, H.; Huang, Z.; Zhu, D.; Tan, C. Brazing ZrB_2-SiC Ceramics to Ti6Al4V Alloy with TiCu-Based Amorphous Filler. *J. Manuf. Process.* **2017**, *30*, 516–522. [CrossRef]
34. Liu, D.; Chen, B.; Jin, G.; Song, Y.; Zhang, Q.; Song, X.; Cao, J. Interfacial Characteristics in CNTs-AgCuTi Systems. *Chin. J. Aeronaut.* **2022**, *35*, 450–460. [CrossRef]
35. Wang, P.; Xu, Z.; Liu, X.; Wang, H.; Qin, B.; Lin, J.; Cao, J.; Qi, J.; Feng, J. Regulating the Interfacial Reaction of $Sc_2W_3O_{12}$/AgCuTi Composite Filler by Introducing a Carbon Barrier Layer. *Carbon* **2022**, *191*, 290–300. [CrossRef]
36. Zhou, X.; Yang, H.; Chen, F.; Han, Y.-H.; Lee, J.; Du, S.; Huang, Q. Joining of Carbon Fiber Reinforced Carbon Composites with Ti3SiC2 Tape Film by Electric Field Assisted Sintering Technique. *Carbon* **2016**, *102*, 106–115. [CrossRef]
37. Sun, Z.; Ma, Y.; Zhang, B.; Zhang, L. Controlling Interfacial Reactions of Ti3SiC2/Ti2AlNb Brazed Joints by Transferring Graphene Layers. *Mater. Sci. Eng. A* **2020**, *771*, 138624. [CrossRef]
38. Zhang, B.; Chang, Q.; Sun, Z.; Li, D.; Pan, H.; Zhang, L. A Concept of Regulating the Distribution of Continuous Brittle Phases by Spatial Division of the Ti3SiC2/Ti2AlNb Brazing Seam. *Mater. Des.* **2022**, *221*, 110941. [CrossRef]
39. Song, Y.; Liu, D.; Hu, S.; Song, X.; Cao, J. Graphene Nanoplatelets Reinforced AgCuTi Composite Filler for Brazing SiC Ceramic. *J. Eur. Ceram. Soc.* **2019**, *39*, 696–704. [CrossRef]
40. Wang, W.; Fan, D.; Huang, J.; Li, C.; Yang, J.; Chen, S. Microstructural Mechanism and Mechanical Properties of Cf/SiC Composite/TC4 Alloy Joints Composite-Diffusion Brazed with TiZrCuNi + TiCp Composite Filler. *Mater. Sci. Eng. A* **2018**, *728*, 1–9. [CrossRef]
41. Zhang, L.X.; Yang, J.H.; Sun, Z.; Liu, X.P.; Feng, J.C. Vacuum Brazing Nb and BN-SiO_2 Ceramic Using a Composite Interlayer with Network Reinforcement Architecture. *Ceram. Int.* **2017**, *43*, 8126–8132. [CrossRef]
42. Zhang, L.X.; Sun, Z.; Chang, Q.; Shi, J.M.; Feng, J.C. Brazing SiO_{2f}/SiO_2 Composite to Invar Alloy Using a Novel TiO_2 Particle-Modified Composite Braze Filler. *Ceram. Int.* **2019**, *45*, 1698–1709. [CrossRef]

Disclaimer/Publisher's Note: The statements, opinions and data contained in all publications are solely those of the individual author(s) and contributor(s) and not of MDPI and/or the editor(s). MDPI and/or the editor(s) disclaim responsibility for any injury to people or property resulting from any ideas, methods, instructions or products referred to in the content.